

Dynamics of transuranic $^{240}\text{Np}^*$ nucleus formed in n-induced reaction

Amandeep Kaur, Gurbinder Kaur, and Manoj K. Sharma*
 School of Physics and Materials Science, Thapar University, Patiala, Punjab

Introduction

The study of neutron induced fission of actinides is of great significance not only to study the nuclear structure and dynamics involved in a reaction, but also to understand the field of reactor physics. This is because fission of such nuclei is helpful in predicting the amount of radioactinides formed [1] which facilitate proper management of nuclear waste. The experimental and theoretical study of reactions involving actinides like Np, Am and Cm etc., are of immense importance to have further insight of the n-induced fission reactions. In view of this, an attempt has been made to study the fission cross-sections of transuranic actinide nucleus $^{240}\text{Np}^*$ formed in $^1_0\text{n} + ^{239}\text{Np} \rightarrow ^{240}\text{Np}^* \rightarrow A_1 + A_2$ reaction. In reference to recent experimental measurements [2], the dynamics involved in n-induced reactions have been explored by studying the fission cross-sections for $^{240}\text{Np}^*$ nucleus using the dynamical cluster decay model (DCM) [3]. For heavy mass nuclei, the deformations and orientation degree of freedom influence the reaction dynamics significantly and need to be taken into consideration. It is relevant to mention here that DCM has been applied to a variety of heavy-ion reactions and role of deformations has been explored in context to different mass regions of the periodic table. Here we intend to extend this feature first time to address the decay pattern of neutron induced reactions, with inclusion of deformation effects up to quadrupole deformations (β_2) in ref. to [3]. The energy range for $^{239}\text{Np}(n,f)$ reaction varies from $E_{lab}=0.625\text{--}20\text{MeV}$. Interestingly, in this energy range, hump in

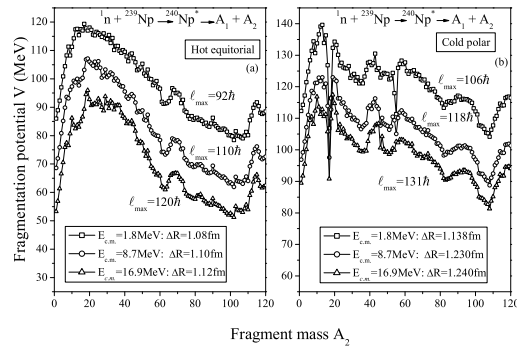


FIG. 1: Variation of fragmentation potential as a function of fragment mass (A_2), for the decay of compound system $^{240}\text{Np}^*$ plotted for (a) cold (polar) and (b) hot (equatorial) configuration.

fission cross-sections representing exceptionally higher fission contribution has been observed at $E_{lab}=1.8\text{ MeV}$, $E_{lab}=8.7\text{ MeV}$ and $E_{lab}=16.97\text{MeV}$ [2]. The experimentally observed cross-sections for these three energies being 1.447b, 1.993b and 2.329b, have been attained successfully (within error limits) by using the only parameter of the model, the neck-length parameter ΔR . The values of the best-fit ΔR are 1.08fm, 1.10fm and 1.12fm for cold interactions and 1.138fm, 1.230fm and 1.240fm for hot interactions for E_{lab} 1.8 MeV, 8.7 MeV and 16.97 MeV respectively. Although we have addressed all the data of [2] but for the space constraints, the results are discussed here at these three energies only.

The Dynamical Cluster-decay Model (DCM)

The DCM [3], based on quantum mechanical fragmentation theory (QMFT), is worked out in terms of collective coordinates of mass (and charge) asymmetries $\eta_A = (A_1 - A_2)/(A_1 + A_2)$ (and $\eta_Z = (Z_1 - Z_2)/(Z_1 + Z_2)$) and relative separation R. With inclusion of deformation and orientation, the compound nucleus decay cross-sections for hot ($T \neq 0$) and

*Electronic address: msharma@thapar.edu

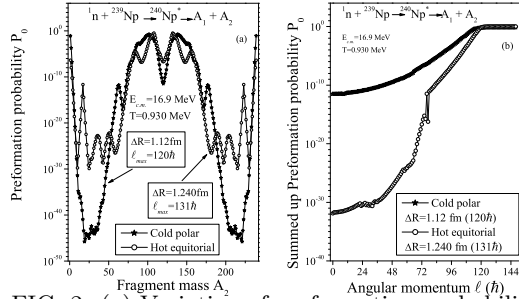


FIG. 2: (a) Variation of preformation probability as a function fragment mass (b) Variation of preformation probability summed-up for $A_2=100-112$ as a function of angular momentum for hot and cold configurations.

rotating ($\ell \neq 0$) nucleus is given as:

$$\sigma = \frac{\pi}{k^2} \sum_{\ell=0}^{\ell_{max}} (2\ell + 1) P_0 P; k = \sqrt{\frac{2\mu E_{c.m.}}{\hbar^2}} \quad (1)$$

The preformation probability (P_0) refers to η -motion and is obtained as solution of the stationary state Schrodinger equation while the penetrability (P) refers to R-motion and is calculated using WKB approximation. Also, ℓ_{max} is the maximum angular momentum fixed for the vanishing of light particle cross-sections i.e. $\sigma_{ER} \rightarrow 0$ and μ is the reduced mass.

Calculations and discussions

The main aim of work presented here is to investigate the effect of deformations and orientations in the decay path of ${}^1_0n + {}^{239}_{91}\text{Np} \rightarrow {}^{240}_{91}\text{Np}^* \rightarrow A_1 + A_2$ reaction. To compare the consistency with results obtained in heavy ion reactions, the fragmentation potential for ${}^{239}\text{Np}(n,f)$ has been studied as a function of fragment mass A_2 for hot and cold configuration. Fig.1(a) represents the variation of fragmentation potential with fragment mass for cold polar configuration at $E_{c.m.}=1.8$ MeV ($T=0.53$ MeV), 8.7 MeV ($T=0.74$ MeV) and 16.9 MeV ($T=0.93$ MeV) while fig.1(b) represents the same for hot equatorial configuration. The comparative analysis of both the figures infer that potential energy surfaces (PES) change considerably when the reaction dynamics transmutes from cold (polar) to hot (equatorial) configuration. Over a varied range of incident energies, the effect of orientational configuration is observed more for intermediate mass fragments (IMF) and fission region whereas the light particles

are not influenced much. Also, the magnitude of fragmentation potential is relatively higher for hot configuration as compared to cold choice of orientation. The role of orientation degree of freedom is also evident from the variation of preformation probability studied as a function of fragment mass and summed-up probability plotted as a function of angular momentum ℓ at highest energy $E_{c.m.}=16.9$ MeV ($T=0.93$ MeV), shown in Fig.2(a) and (b) respectively. Fig.2(a) suggests that the fragment mass distribution is asymmetric for both choices of orientation, being relatively more asymmetric for cold polar approach. Although the orientational configuration affects the preformation probability, the favorable fission fragments for both choices remain the same i.e. the fragments, $A_2=100-112$ and complementary heavy mass fragments are the main contributors towards fission cross-sections. From Fig. 2(b) it is inferred that, summed up P_0 also behaves differently as a function of angular momentum for hot and cold configuration, being much lower for earlier one. The fission cross-sections calculated at the above mentioned energies are found to have descent agreement with the experimental data [2]. In summary, for neutron induced reactions, the deformation and orientation effects are prominent for fission and IMF region although the contributing fragments remain unaffected by the choice of orientation degree of freedom. The calculated fission cross-section find nice agreement with available data.

Acknowledgement

The financial support from DST, New Delhi is gratefully acknowledged.

References

- [1] V. V. Desai et al. Phys. Rev. C **88**, 014613 (2013)
- [2] A. Czeszumaska et al. Phys. Rev. C **87**, 034613 (2013)
- [3] R. K. Gupta et al., *J. Phys. G*, **31**, 631, (2005); G. Kaur and M. K. Sharma, *Nucl. Phys. A*, **884**, 36, (2012); *ibid Phys. Rev. C*, **87**, 044601. (2013).